scientific reports

Check for updates

OPEN

Prediction and reliability analysis of rigid pipeline response in soft soil using improved particle swarm neural network

Laifu Song, Shun Zhang, Jun Wang✉, Hongtao Fu & Jiayu Cai

Pipelines in soft soil are prone to deformation and failure under traffic loads. Therefore, it is highly important to accurately characterize the dynamic response of pipelines under traffic loads and reasonably evaluate their operational status. First, for rigid pipelines, a Dload subroutine is written in the FORTRAN language to accurately characterize traffic loads, and a 3D numerical analysis model of the rigid pipe–soil system is established using ABAQUS software to simulate the dynamic response of rigid pipelines in soft soil under traffic loads. The simulation results are validated against data from field tests. Second, an improved particle swarm optimization (PSO) algorithm is introduced to optimize the weights and thresholds of a backpropagation neural network (BPNN). An improved PSO-BPNN method for predicting the dynamic response of pipelines is proposed, and the accuracy and applicability of the method are verified. Finally, using the prediction model, a reliability analysis is conducted on the dynamic response of rigid pipelines in soft soil under traffic loads. The results show that compared with smaller-diameter pipelines, larger-diameter pipelines exhibit lower axial stress and vertical displacement, with more concentrated distributions. During pipeline construction, larger-diameter pipelines should be chosen whenever possible to reduce the adverse impact of factors such as traffic loads on the dynamic response of pipelines. These research results provide a new theoretical basis and technical support for enhancing the reliability of rigid pipelines in soft soil and conducting in-depth safety assessments of pipelines under traffic loads.

Keywords Traffic load, Rigid pipe, Soft soil foundation, DLOAD subroutine

Pipelines, along with railways, highways, air transportation, and water transportation, are known as the five major means of transportation. They are important infrastructures for urban development as well as vital "lifeline engineering" for improving people's quality of life and ensuring social stability and security. By the end of 2023, the total mileage of various types of pipelines in China had exceeded 3.5 million kilometres. Among them, rigid pipelines have become one of the main types of pipelines for oil and gas as well as water supply and drainage applications because of their advantages of small deformation, stable performance, long service life, ease of repair, and wide applicability.

For a long time, pipeline network construction in China has faced the problem of "emphasizing construction while neglecting maintenance." In addition, since pipelines are concealed structures, it is difficult to detect damaged or destroyed areas in a timely manner during pipeline construction and operation. Moreover, with the rapid social and economic development and the accelerated urbanization in China, underground pipeline networks often cross soft soil layers such as mud and swamps. These layers have a high water content, poor permeability, low strength, and high compressibility, and their strength decreases sharply when disturbed, resulting in poor geotechnical properties. Pipelines laid on soft soil foundations are highly susceptible to structural issues such as settlement, warping, and cracking. In addition, with the gradual expansion of highway and railway transportation networks, increasingly more underground pipeline networks intersect with surface transportation lines. Under high traffic volume and frequency, pipeline foundations are prone to long-term uneven settlement and deformation, altering the pipe-soil interaction and further aggravating pipeline deformation, damage, and failure.

College of Civil Engineering and Architecture, Wenzhou University, Wenzhou 325035, China. ✉email: 20210115@wzu.edu.cn

Many researchers have studied the mechanical response of buried pipelines under traffic loads using theoretical analyses, model tests, and numerical simulations. In the 1970s, Parmelee and Ludtke[1] proposed the Winkler model for beams on elastic foundations. Later, Rajani and Tesfamariam[2], based on the Winkler theory, developed a model for calculating the longitudinal force on pipelines considering temperature and internal pressure. Li et al.[3] used the Winkler model to propose a simplified model for calculating pipeline longitudinal force and verified it through numerical simulations and field tests. Fernando and Sérgio[4] systematically studied the deformation patterns of pipelines in cohesionless soil under moving loads through centrifuge model tests and modified the theoretical formulas of Spangler and Boussinesq. Wang and Xiao[5] conducted laboratory model tests to study the relationships between the mechanical properties and deformation characteristics of surrounding soil and a pipeline and verified the model test results using theoretical formulas. Based on laboratory model tests, Shi et al.[6] analysed the inherent relationship and influencing factors of road surface collapse under pipeline leakage and traffic loads based on laboratory model tests. Hyodo and Yasuhara[7] showed through field tests that the additional stress on soil by traffic loads can be represented by a pulse curve. Li[8] simplified the traffic load model and analysed the dynamic response of buried pipelines using numerical simulation software. Xie[9] used a half-wave sinusoidal curve to characterize the fluctuation of traffic loads by modulating the amplitude function in ABAQUS software and analysed the dynamic response of concrete pipelines under traffic loads. However, traffic loads vary with time and space and exhibit a certain degree of randomness. Xu et al.[10] established a vehicle–soil–pipeline model, which used the temporal variation of loads in a specific area to describe the running process of a vehicle, and they studied the mechanical response of large-diameter pipelines. Jiang et al.[11] used ADAMAS to extract the amplitude of moving loads and employed finite element software to simulate the dynamic response of a pipeline under traffic loads. It is clear that the existing research has mostly focused on rigid pipelines in sand or loess, and few studies have investigated rigid pipelines in soft soil. Traffic loads have uncertainties in magnitude, direction, and points of application, so it is clearly inaccurate to simplify them as static or pulse loads. Traditional deterministic analysis methods such as model tests and numerical simulations have certain limitations and are unable to scientifically and rationally characterize the influence of various uncertainty factors on the mechanical response of buried pipelines and perform quantitative evaluation.

In summary, to address the vulnerability of pipelines in soft soil to deformation and failure under traffic loads, the present study developed a traffic load subroutine using ABAQUS software and established a 3D numerical analysis model for a rigid pipeline–soil system to accurately simulate the dynamic response of rigid pipelines in soft soil under traffic loads. In view of the defects of the traditional backpropagation neural network (BPNN), where the selection of initial weights and thresholds can easily lead to the local optimum of the trained model, the present study used an improved particle swarm optimization (PSO) algorithm to optimize the weights and thresholds of the BPNN, improving the prediction accuracy and efficiency of the model. The accuracy and applicability of the method were verified through actual engineering cases. A reliability analysis of the dynamic response of rigid pipelines in soft soil under traffic loads was performed using the prediction model, and the differences in the dynamic response reliability of rigid pipelines with different pipeline diameters under traffic loads were compared.

Methods for pipeline dynamic response prediction and reliability analysis

BPNN algorithm

The BPNN is an error backpropagation neural network that mainly consists of two learning processes, i.e., forward propagation of the input signal and backpropagation of the error signal. Its structure is divided into three layers: an input layer, a hidden layer, and an output layer. During forward propagation, the input data flow from the input layer through the hidden layer and finally to the output layer, where the neurons in the previous layer affect the neurons in the next layer, and the neurons are determined by inputs, activation functions, and thresholds. When the error in the output layer is large, backpropagation is performed, and the objective function with the minimum error is obtained by repeatedly modifying and adjusting the weights and thresholds of the neurons (Fig. 1).

The BPNN algorithm is a nonlinear space mapping method for solving nonlinear optimization problem. It has strong capabilities in nonlinear mapping, generalization, and fault tolerance. However, this method is based on the gradient descent principle, resulting in slow convergence and issues with local minima, which can cause the algorithm to be easily trapped in local extrema, severely limiting its application.

Improved PSO algorithm

PSO is an intelligent global optimization algorithm. It implements swarm iteration by simulating bird flock foraging, searching for the optimal region in the space among swarm particles, and eventually obtaining the optimal particle in the target solution space. The solution of each optimization problem is a particle, that is, a flying bird in the space discovering and exploring the individual and global optimal solutions. During the training of model parameters in the PSO-BPNN algorithm, the network weights and thresholds are treated as particles, and particles can uniquely determine the network weights and thresholds. The goal of optimizing the network is ultimately achieved by continuously updating the particle positions, i.e., the weights and thresholds of BPNN. However, the inertia weight in the standard PSO algorithm is linearly related to the number of particle swarm iterations, and the integration of PSO with BPNN can easily cause the "clustering" of the particles in the particle swarm, leading to the "prematurity" of particles and the calculation result being trapped in local minima.

Therefore, to overcome the above problems and enhance the global search capability of the whole algorithm, the standard PSO algorithm is improved by introducing two variables, the evolution degree and the aggregation degree, into the particle swarm to enable the dynamic change in the inertia weight. The two variables are expressed as follows:

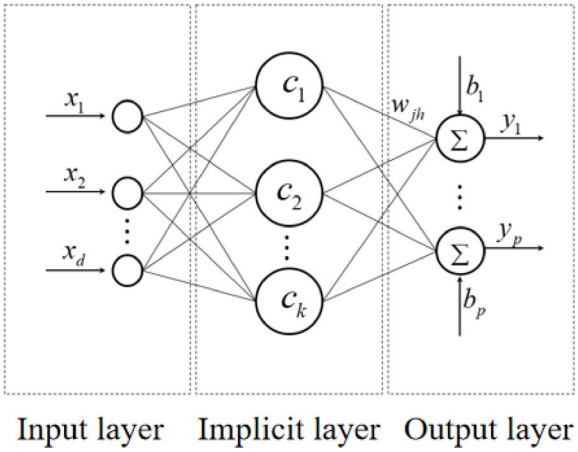

Fig. 1. Schematic diagram of the BPNN structure. This figure was drawn using Microsoft PowerPoint 2016. (Software: Microsoft PowerPoint 2016)

$$e = \frac{E_{j(t)}}{E_{j(t-1)}} \tag{1}$$

$$d = \frac{M \cdot E_{j(t)}}{\sum_{J=1}^{M} E_{j(t-1)}} \tag{2}$$

where e is the evolution degree of the particle swarm, characterizing the degree of evolution and convergence of the particle swarm; at the beginning of the iteration, it has a small value, indicating a fast evolution speed. Later, its value decreases, and the evolution speed slows down; when this value becomes 1 and remains unchanged, the algorithm has stagnated or found an optimal solution. $E_{j(t-1)}$ represents the particle fitness of the global optimal solution in the previous iteration, and $E_{j(t)}$ is the particle fitness of the current global optimal solution. a is the aggregation degree of the particle swarm, with a smaller value indicating a more dispersed particle distribution; when it is 1, all the current particles are optimal, and the particle swarm has aggregated into one point. M is the particle swarm size, also known as the number of particles.

Implementation steps of the improved PSO-BPNN

The specific steps of the improved PSO-BPNN algorithm are as follows:

(1) Initialize the BPNN by determining the number of neurons in the input layer, hidden layer and output layer.
(2) Determine the particle swarm size M, the dimension n, and the velocity vector and the displacement vector of the particles in the initial particle swarm.
(3) Input the sample data and perform the BPNN forward propagation calculation to obtain the training error and the fitness values of the particles.
(4) Compare the fitness values to determine the individual optimal solutions of all particles and the global optimal solution.
(5) Iteratively update the individual optimal solutions of all particles and the global optimal solution through the BPNN algorithm.
(6) Continuously update the velocity vectors and position vectors of all particles in the particle swarm.
(7) To determine if the termination condition is met, check whether the number of iterations satisfies the required criterion or whether the mean square error of the objective optimization function meets the accuracy threshold.

The specific process of the improved PSO-BPNN algorithm is shown in (Fig. 2). This method integrates the advantages of the BPNN and PSO algorithms. By improving the standard PSO algorithm and combining it with the BPNN algorithm, the "clustering" of particles in the particle swarm can be effectively prevented, thus overcoming the "prematurity" of particles and ultimately making the optimal solution a global optimum.

Reliability analysis of pipeline response based on BPNN with improved PSO

The reliability analysis of the dynamic response of pipelines based on the BPNN with improved PSO includes three main parts. (1) Generating sample data: experimental design methods such as importance sampling, Latin hypercube sampling, and factorial design are used to generate sample data that can uniformly cover the entire random variable interval, thereby overcoming the issue of the large sample size in Monte Carlo simulation (MCS) methods, reducing the number of samples, and improving the computational efficiency. (2) Based on the BPNN prediction model with improved PSO, which fully integrates the advantages of improved PSO and BPNN, the prediction model is established using a nonlinear method with strong applicability, high fault tolerance, and

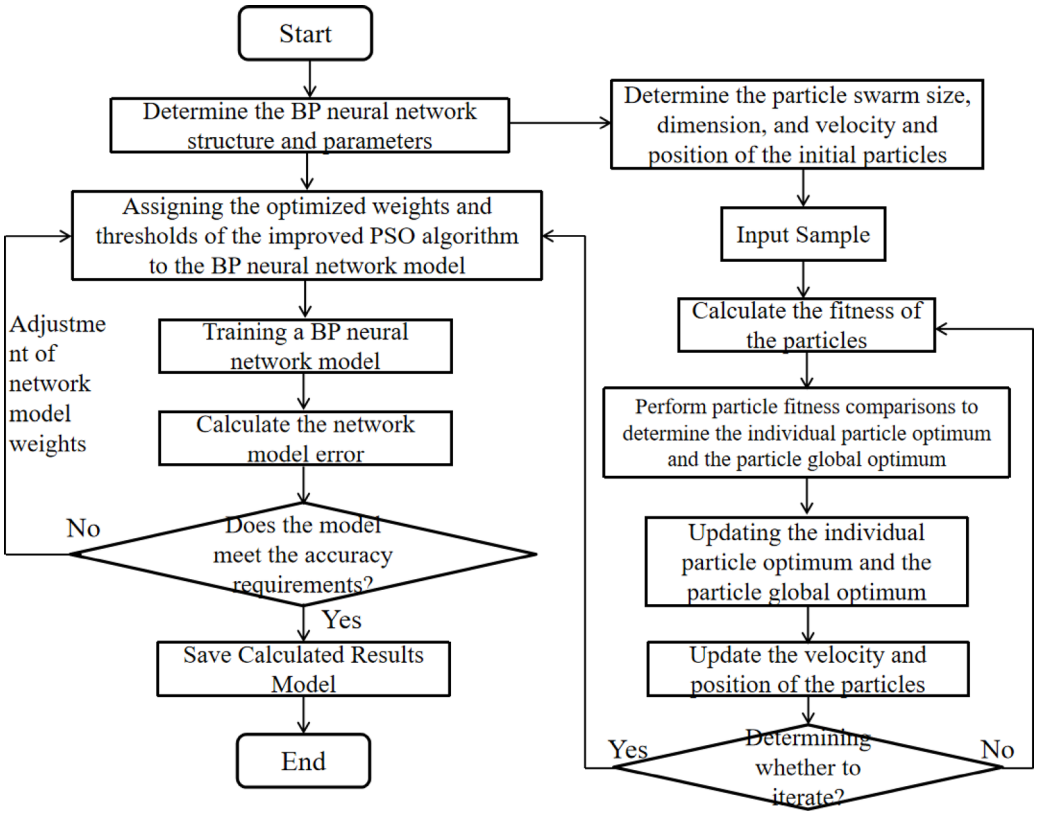

Fig. 2. Flowchart of the improved PSO-BPNN algorithm. (Software: Microsoft PowerPoint 2016)

high global search capability. (3) Calculating system reliability: based on the prediction model, the reliability of the dynamic response of rigid pipelines under traffic loads is calculated using the MCS method for random variable sampling. Figure 3 shows the flowchart for the reliability analysis of the dynamic response of pipelines based on the BPNN with improved PSO.

Numerical example

Calculation models and parameters

An actual engineering project is used for the calculation example. The project is located in the Wenzhou Technology Development Zone, Zhejiang Province. The soil layer consists of dredger-filled soft soil, which is highly compressible, underconsolidated, and has a high water content. The overall size of the model is more than five times the size of the pipeline, meeting the requirements for the model boundary effect. The calculation model has a length, width, and height of 20 m, 6 m, and 8 m, respectively. The pipeline is a made of ductile iron with a length of 6 m. C3D8R elements are used to mesh both the rock–soil mass and the pipeline, with the rock–soil mass having a grid size of approximately 0.45 m, which is refined to 0.1 m for the load area, and the pipeline having a grid size of 0.05 m, resulting in a total of 88,510 nodes and 76,560 elements, as shown in (Fig. 4). The contact interface model can effectively describe the nonlinear response of pipe-soil interaction. Therefore, in this section, the soil is modeled using continuum solid elements, and the general contact algorithm in ABAQUS is adopted to simulate the pipe-soil interaction. The normal direction is defined with a hard contact formulation, while the tangential direction employs a penalty-based friction formulation. The bottom of the model is fully fixed, and the normal displacement of the lateral sides is constrained. The Mohr–Coulomb model is used to characterize the elastic–plastic mechanical behaviour of the rock–soil mass, and the Ramberg–Osgood model is used to characterize the stress–strain relationship of the pipeline material, with a yield stress of 450 MPa. The material parameters are shown in (Table 1).

Since the burial depth and vehicle load have a great impact on buried pipelines in soft soil, in the present study, the two parameters are discretized to analyse the mechanical response of rigid pipelines with different diameters under traffic loads. The sample parameters are generated using the Latin hypercube sampling method. Studies have shown[12–14] that a sample size of $N = 15\ D$ (D represents the number of parametric variables; $D = 2$ in this example) can achieve satisfactory calculation results, with the test sample size being 15 or 20. To better verify the accuracy of the method, the sample size in this numerical example is set to 60 (which is greater than $N = 15\ D = 30$), and 20 sets of data are taken as test samples. The sample interval for parameters with normal distribution and lognormal distribution is $(\mu_x - 4\sigma_x, \mu_x + 4\sigma_x)$ (μ_x, σ_x are the mean and standard deviation of the random variable parameter, respectively).

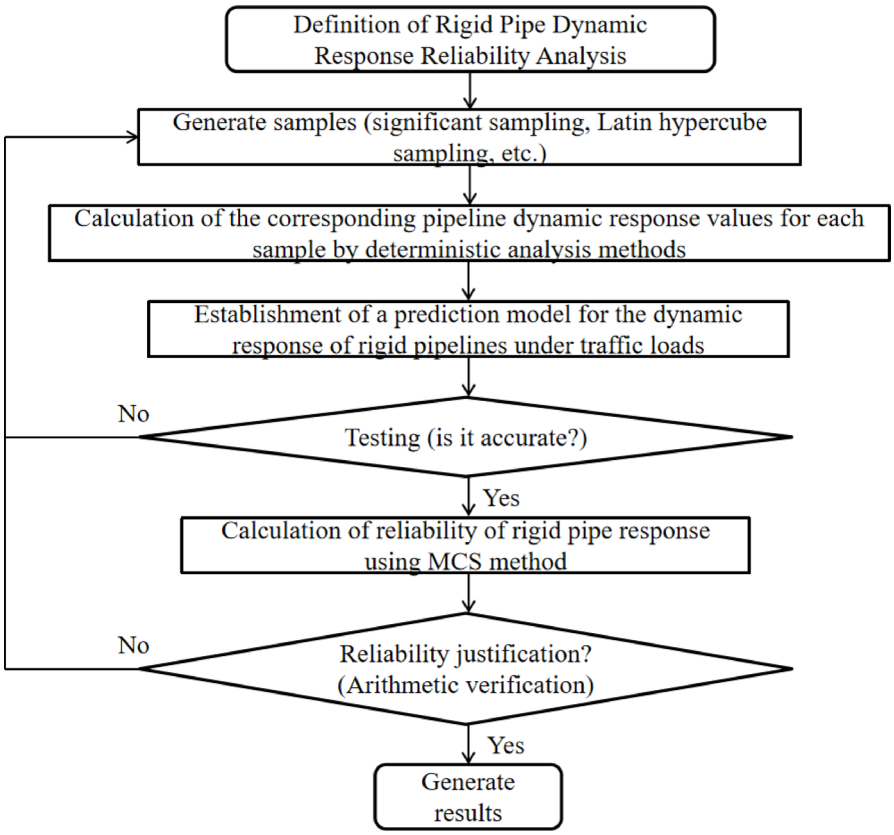

Fig. 3. Flowchart for the reliability analysis of the dynamic response of pipelines based on BPNN with improved PSO. (Software: Microsoft PowerPoint 2016)

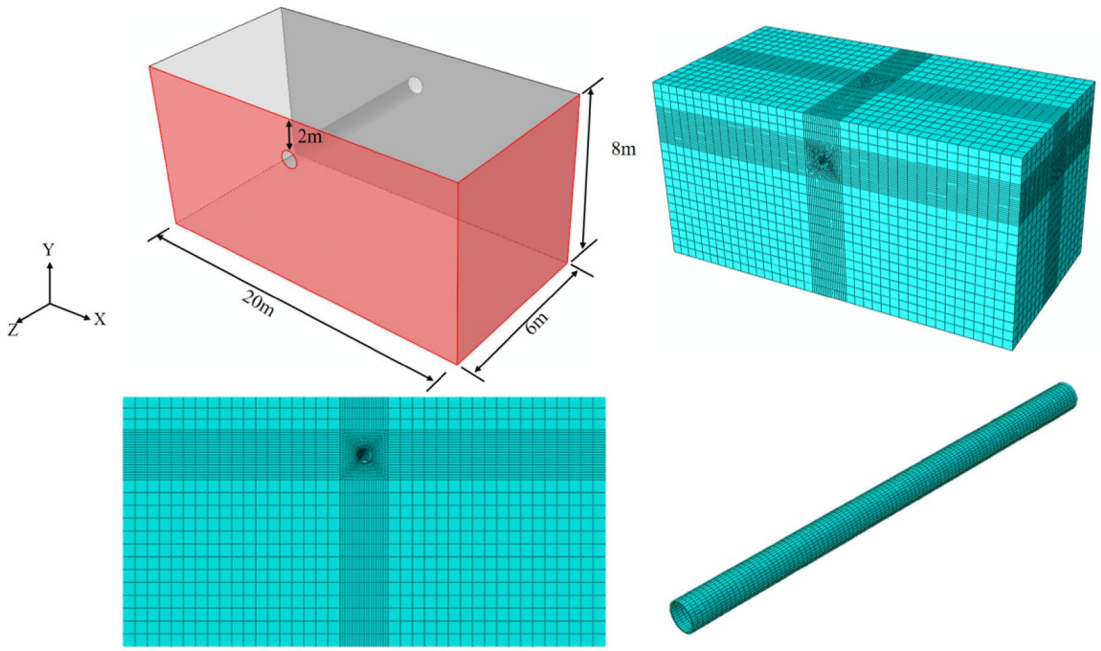

Fig. 4. Schematic diagram of the finite element model.(Software: Abaqus/CAE 2020).

Material	Density (kg/m³)	Elastic modulus (MPa)	Poisson's ratio μ	Internal friction angle (°)	Cohesion (KPa)
Soft soil	1850	10	0.3	8	5.0
Ductile iron pipe	7300	1.6×10^5	0.3	–	–

Table 1. Material parameters.

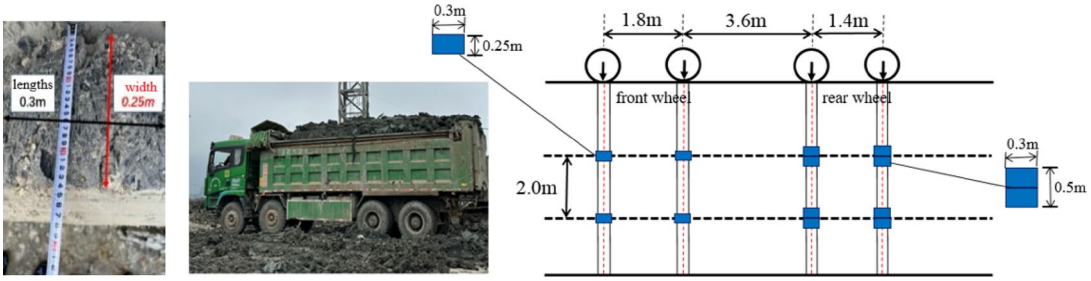

Fig. 5. Schematic diagram of the vehicle load model. (Software: Microsoft PowerPoint 2016)

Traffic load model

The existing studies usually simplify vehicle loads as static loads or half-wave sinusoidal curves[7]. This method can only be used to apply loads in specific areas and is unable to realistically represent dynamic changes in the magnitude, direction, and application points of traffic loads of running vehicles. In this study, a Dload subroutine was developed and used in combination with ABAQUS software to accurately simulate the real process of running vehicles.

During the running process of a vehicle, the pressure exerted by the vehicle on the road surface can be characterized by the contract pressure between the wheels and the ground. Based on actual engineering vehicles and field measurements, the basic dimension of the contact area between a single wheel of a large freight vehicle and the ground is 0.3×0.25 m2. The vehicle has a total of four axles and 12 wheels, with a total contact area of 0.9 m2 between the wheels and the ground, The vehicle width of the vehicle is 2 m, the wheelbase of the front axle is 1.8 m, and the wheelbase of the rear axle is 1.4 m. as shown in (Fig. 5).

Validation of numerical simulation results

Vehicle loads are applied to the top of the model, and the vehicle travels straight from the left end to the right end of the model. During the driving process of the vehicle, the pipeline undergoes four processes (Steps 1 to 4). The circumferential and axial stresses during the driving process are extracted and compared with the field-measured values, as shown in (Fig. 6).

Figure 6 shows the steps. Step 1: The pipeline stress gradually increases as the vehicle moves to the right at a constant speed, and the axial and circumferential stresses of the pipeline reach their first peaks when the front axle in the front of the vehicle is directly above the pipeline. Step 2: When the front axle leaves the top of the pipeline, the pipeline stress decreases to some extent. However, the pipeline stress reaches the second peak when the rear axle in the front of the vehicle is directly above the pipeline. Due to the short distance between the front and rear axles, a certain stress accumulation effect occurs, making the second peak slightly higher than the first peak. Step 3: When the rear axle in the front of the vehicle leaves, the circumferential and axial stresses of the pipeline decline sharply, and when the rear of the vehicle drives above the pipeline, both circumferential and axial stresses reach the maximum peaks. Since the weight of the vehicle is mainly concentrated on the rear of the vehicle and the distance between the front and rear axles in the rear of the vehicle is small, the two axles can be considered to act at the same time. Step 4: The pipeline stress gradually decreases after the rear axle in the rear of the vehicle moves away from the top of the pipeline until it stabilizes in the numerical simulation. The numerical simulation results generally agree with field measurement data, with maximum errors of 8.52% and 5.39% for circumferential and axial stresses, respectively.

We select one set of working conditions and extract the pipeline axial stresses from numerical simulations and field measurements for comparison. As shown in (Fig. 7). The figure shows that, the axial stress along the axis of the pipeline from numerical simulations is in high agreement with that from field measurement. Therefore, the traffic load model and the numerical calculation model developed in this study have high accuracy.

Prediction and reliability analysis of the mechanical response of the pipeline

By performing deterministic numerical simulations on 60 sets of sample data, the dynamic response of the rigid pipeline in soft soil under traffic loads, such as the stress-strains and displacement of the pipeline, are obtained (Fig. 8). Here, the vertical displacement of the rigid pipeline is taken as an example to perform statistical analysis on the 60 sets of randomly obtained sample data. With the pipeline burial depth and vehicle load as inputs, the vertical displacement of the rigid pipeline is predicted using the BPNN with improved PSO. Figures 9, 10 compares the measured and predicted values using the training and test set samples, respectively. As shown in the figure, the predicted values for both the training and test sets exhibit a high degree of consistency with the

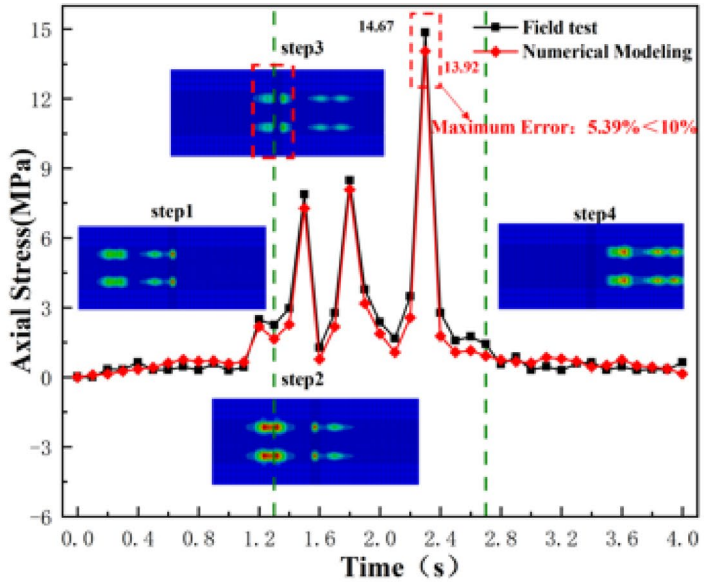

(a)

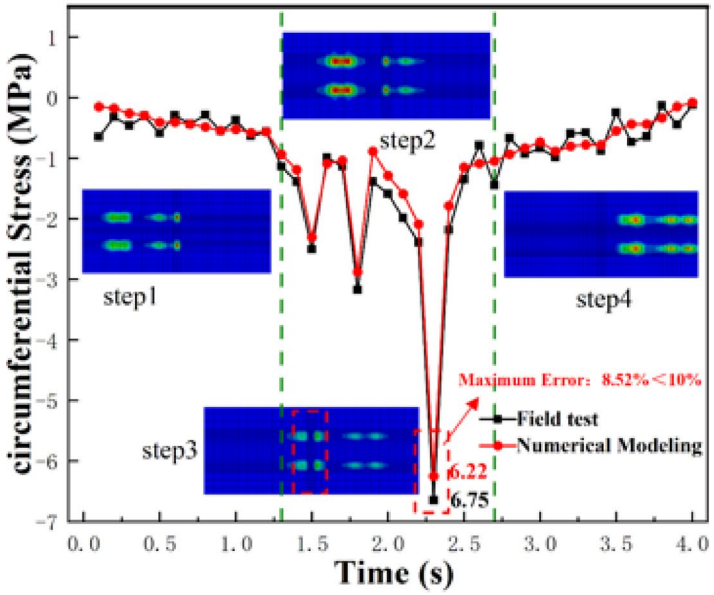

(b)

Fig. 6. Comparison of circumferential and axial stress time history curves of the pipeline between field tests and numerical simulations. (3D model: Abaqus/CAE 2020; Data visualization: OriginLab Origin 2018, 64-bit version)

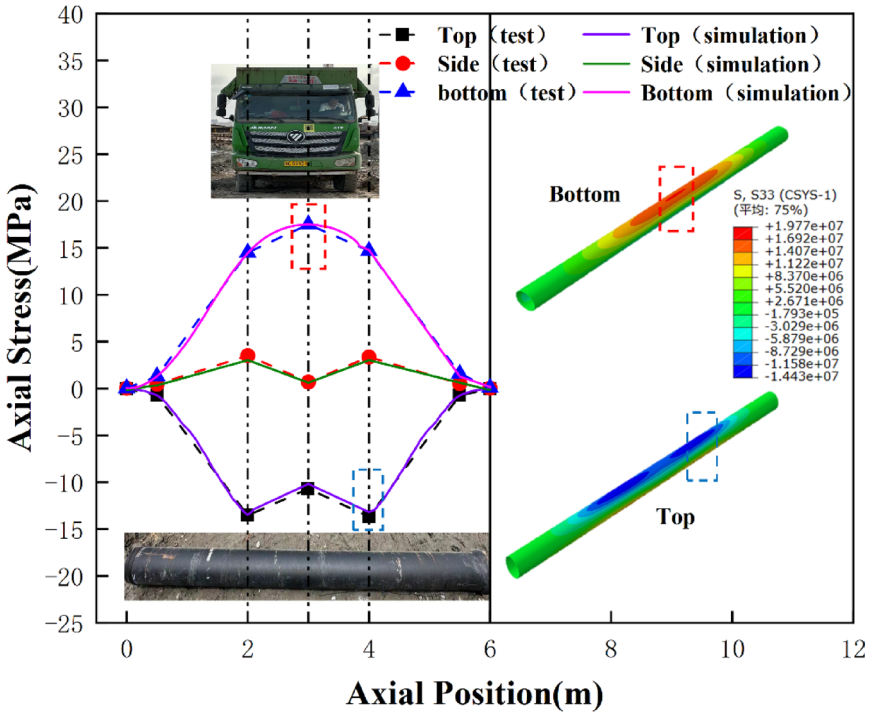

Fig. 7. Comparison of axial stresses along the pipeline axis between field tests and numerical simulations. (3D model: Abaqus/CAE 2020; Data visualization: OriginLab Origin 2018, 64-bit version)

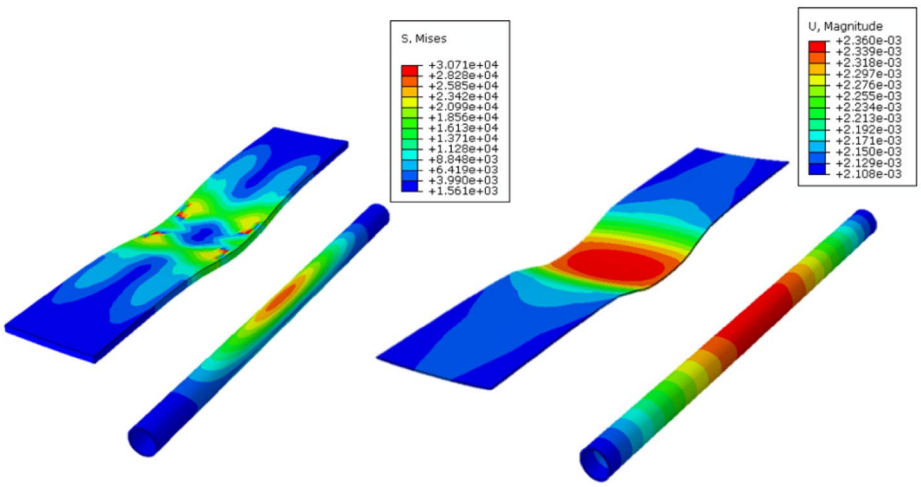

Fig. 8. Contours of pipeline stress and displacement. (Software: Abaqus/CAE 2020)

measured values, with data points densely distributed along the diagonal. The training set achieves an R^2 of 0.9839 (ERMS = 0.08288), while the testing set yields an R^2 of 0.9541 (ERMS = 0.12615), indicating that the model does not exhibit significant overfitting during training. The absence of systematic bias and the uniform distribution of data points on both sides of the diagonal further validate the effectiveness of the improved PSO-BPNN model in capturing the nonlinear characteristics of rigid pipeline responses in soft soil. The model demonstrates reliable generalization capability for unknown conditions while maintaining high accuracy in the training set.

Table 2 lists the evaluation metrics for the prediction results corresponding to the training and test sets, respectively. E_{RMS} values are all less than 0.2, and the goodness of fit R^2 values are greater than 0.95, indicating an overall small prediction error and a high prediction accuracy. As shown in the table, the prediction accuracy of the training set is slightly higher than that of the test set, indicating that the established prediction model can fully identify the sample data characteristics of the training set, has strong generalizability, and can be well applied to prediction of the dynamic response of rigid pipelines in soft soil under traffic loads.

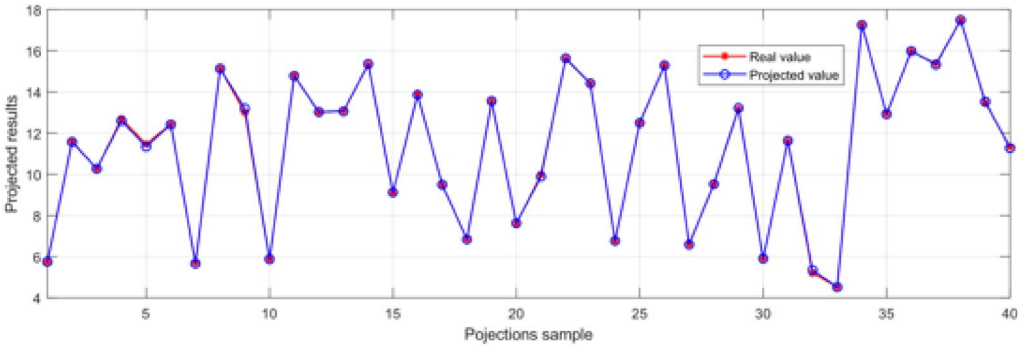

(a)

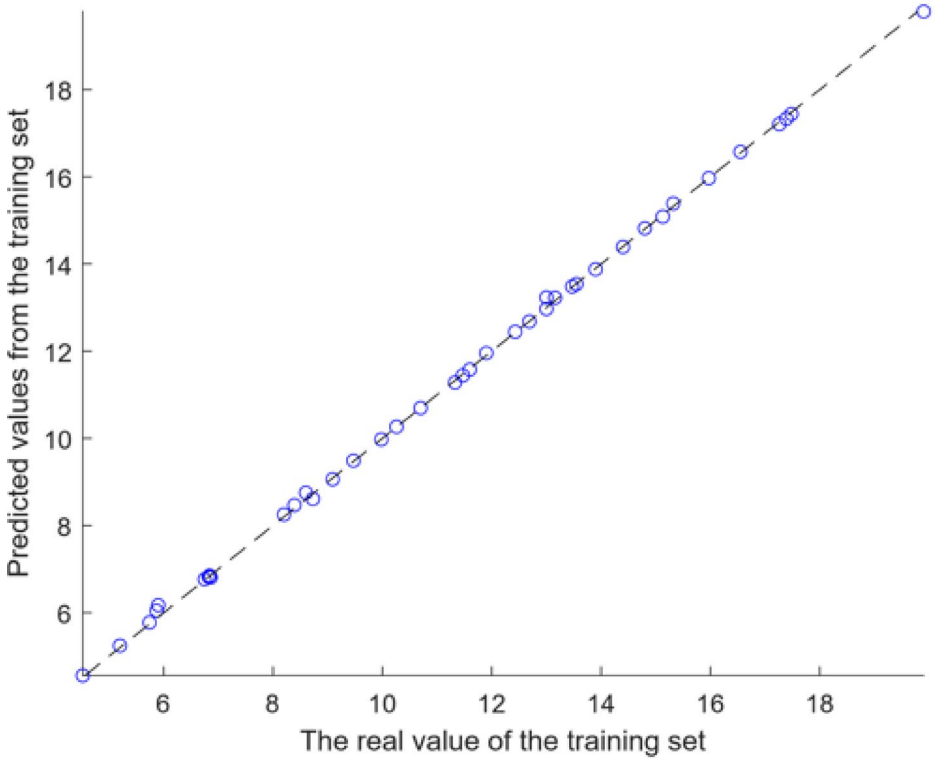

(b)

Fig. 9. Comparison of measured and predicted results using the training sample set. (Software: OriginLab Origin 2018, 64-bit version)

Based on the prediction model established above, a reliability analysis is performed on the dynamic response of the rigid pipeline in soft soil under traffic loads. The calculation results are shown in (Figs. 11, 12). Figure 11 shows that, under the same loads and burial depth, a smaller pipe diameter leads to a more widely distributed axial stress and a lower concentration of stress values; conversely, a larger pipe diameter results in a more narrowly distributed axial stress and a higher concentration of stress values. The distribution is relatively concentrated. The above conclusion is further verified from the perspective of pipeline vertical displacement in

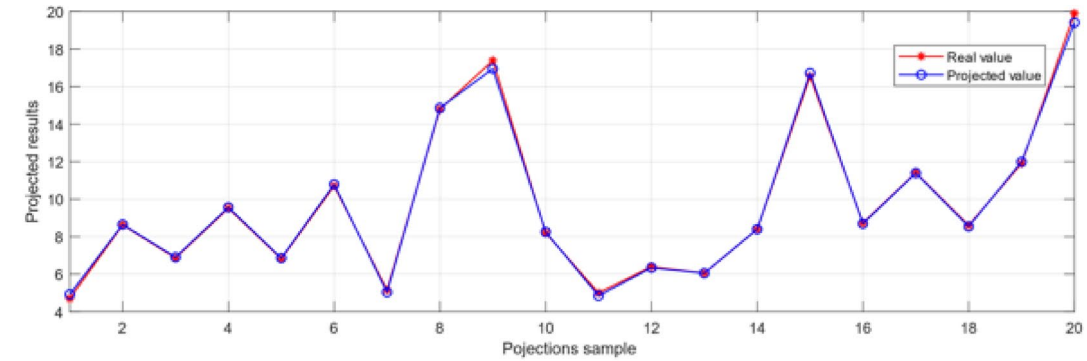

(a)

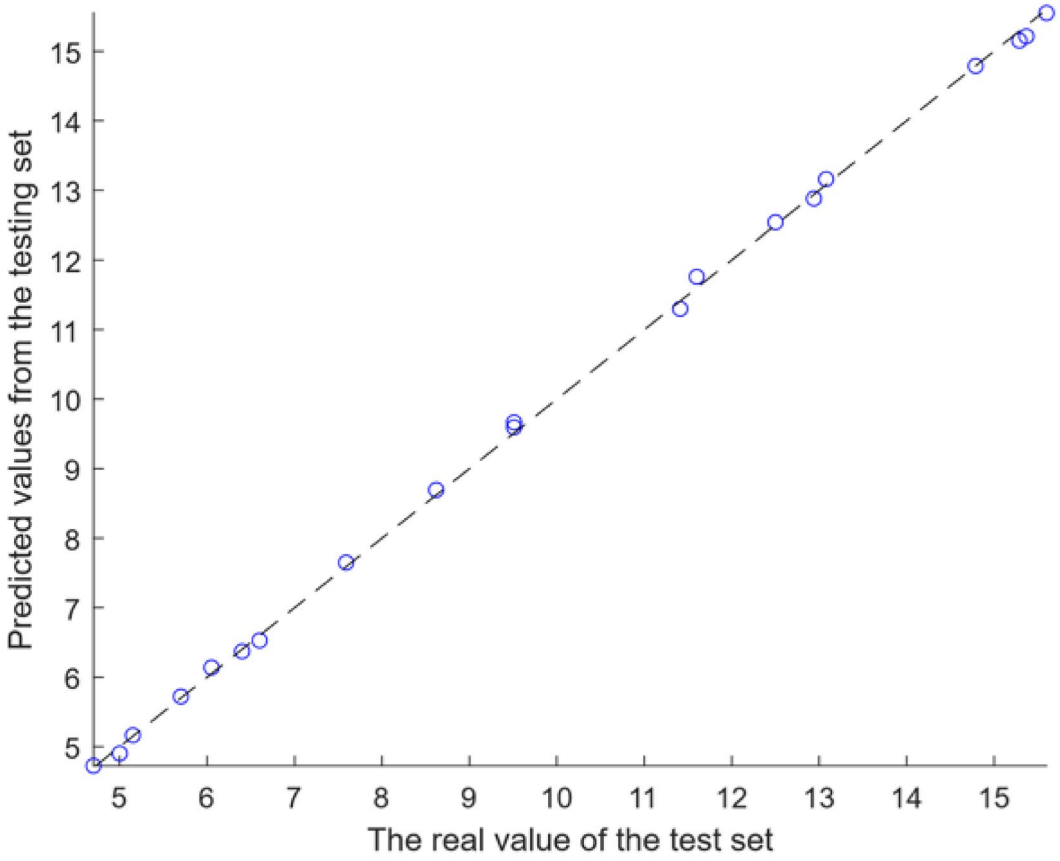

(b)

Fig. 10. Comparison of measured and predicted results using the test sample set. (Software: OriginLab Origin 2018, 64-bit version)

Dataset	Sample size	E_{RMS}	R^2
Training set	40	0.08288	0.9839
Test set	20	0.12615	0.9541

Table 2. Prediction accuracy of the vertical displacement of the rigid pipeline.

(Fig. 12). Under the same loads and burial depth, larger-diameter pipelines have smaller vertical displacement with more concentrated distribution than smaller-diameter pipelines. Therefore, under the same load and burial depth, compared with smaller-diameter pipelines, larger-diameter pipelines experience lower force-induced displacement and are less likely to fail. During pipeline construction, given that economic and geological conditions are met, it is recommended to choose larger pipe diameters to reduce the unfavourable impact of factors such as traffic loads on the dynamic response of rigid pipelines.

Conclusions

In this study, based on ABAQUS software, the DLOAD subroutine was written in the FORTRAN language to accurately characterize the traffic load, and a 3D numerical analysis model for rigid pipeline–soil system is established to simulate the dynamic response of rigid pipelines in soft soil under traffic loads. The simulation results are compared with data from field tests to verify the accuracy of the method. Second, to address the defect that the selection of initial weights and thresholds in a traditional BPNN easily leads to the local optimum using the trained model, an improved PSO is used to optimize the weights and thresholds of the BPNN, improving the prediction accuracy and efficiency of the model. The feasibility and accuracy of the proposed method in predicting the dynamic response of pipelines are verified through an actual case example. Finally, based on the above prediction model, a reliability analysis is conducted on the dynamic response of rigid pipelines in soft soil under traffic loads. Under the same traffic loads and burial depth, compared with smaller-diameter pipelines, larger-diameter pipelines have lower axial stress and vertical displacement, with more concentrated distributions. During pipeline construction, as long as economic and geological conditions are met, large-diameter pipelines should be chosen to reduce the adverse impact of factors such as traffic loads on the dynamic response of pipelines.

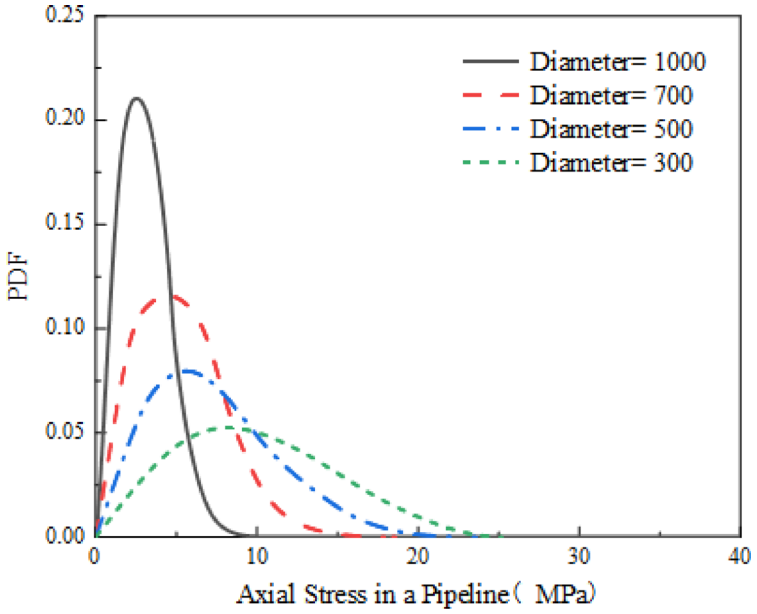

(a)

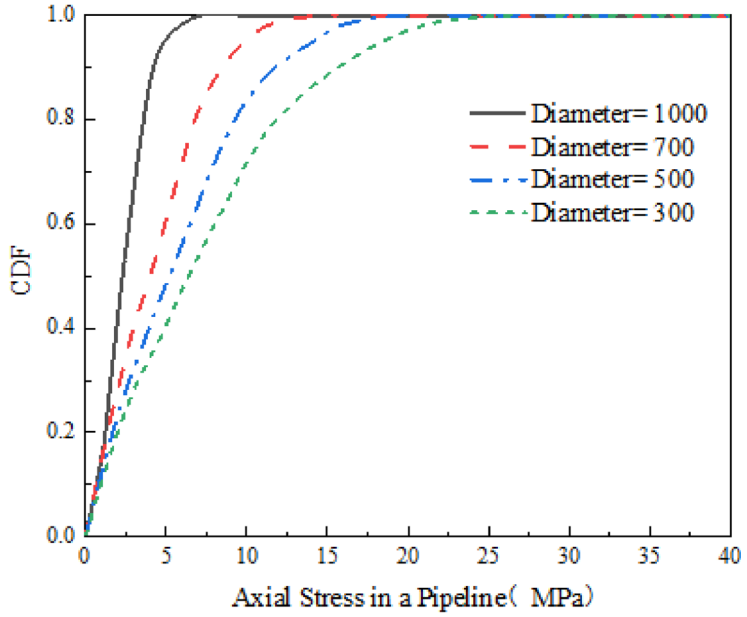

(b)

Fig. 11. Curves of the probability density function and cumulative distribution function of pipeline axial stress. (Software: OriginLab Origin 2018, 64-bit version). (**a**) The probability density function of pipeline axial stress. (**b**) The cumulative distribution function of pipeline axial stress.

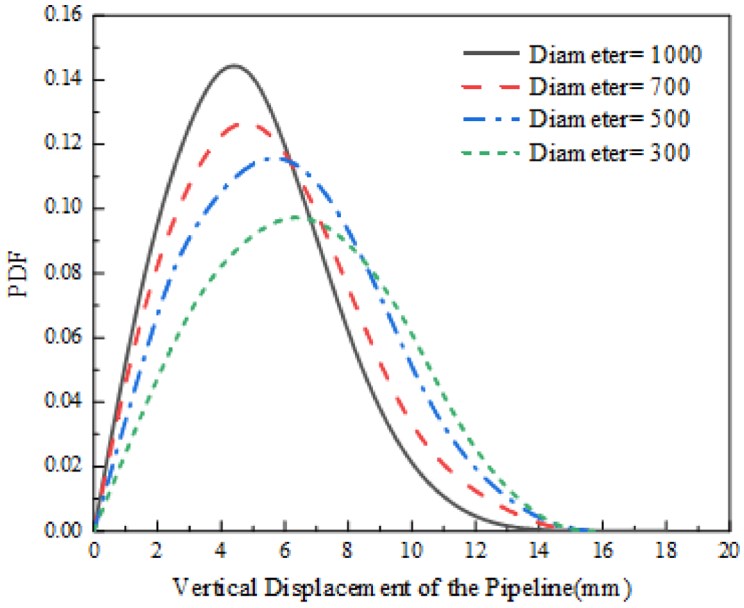

(a)

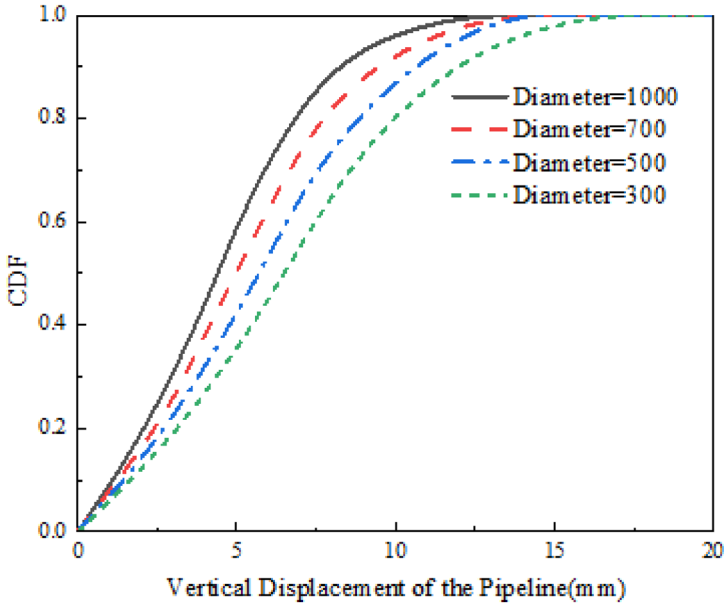

(b)

Fig. 12. Curves of the probability density function and cumulative distribution function of pipeline vertical displacement. (Software: OriginLab Origin 2018, 64-bit version). (**a**) The probability density function of pipeline vertical displacement. (**b**) The cumulative distribution function of pipeline vertical displacement.

Data availability

The datasets supporting the conclusions of this study are provided under license by Wenzhou University and are not publicly accessible. Access to these data may be granted to qualified researchers upon written request to the authors, subject to approval by Wenzhou University. For inquiries, please contact Professor Laifu Song at songlaifu_jia@wzu.edu.cn.

Received: 5 March 2025; Accepted: 2 June 2025
Published online: 02 July 2025

References

1. Parmelee, R. A. & Ludtke, C. A. *Seismic soil-structure Inters Action of Buried Pipelines [A] / / Proc Eeding of US National Conf Earthq Eng[C]* 406–415 (EERI, 1975).
2. Rajani, B. & Tesfamariam, S. Uncoupled axial, flexural, and circumferential pope-soil interaction analyses of partially supported jointed water mains. *Can. Geotech. J.* **41** (6), 997–1010 (2004).
3. Li, H., Han, G. & Wang, X. Calculation of longitudinal stress of buried pipeline under traffic load. *Chin. J. Undergr. Space Eng.* **18** (5), 1511–1520 (2022).
4. Fernando, S. & Sérgio, T. Centrifuge and numerical modeling of moving traffic surface loads on pipelines buried in cohesionless soil. *Transp. Geotechnics.* **23**, 100340 (2020).
5. Jiayong Wang. Numerical modeling on mechanical properties of shallow-buried HDPE pipe protected with geogrids. *J. Hebei Univ. Technol.* **51** (2), 91–96 (2022).
6. Gang, S. et al. Model experiments on ground collapse under traffic roads. *Chin. J. Undergr. Space Eng.* **16** (4), 1202–1209 (2020).
7. Hyodo, M. & Yasuhara, K. Analytical procedure for evaluating pore-water pressure and deformation of saturated clay ground subjected to traffic loads. *Proc 6th International Conference on Numerical Methods in Geomechanics, Publ Rotterdam: A A Balkema* 653–658 (1988).
8. Xun Li. *Analysis on Mechanical Characteristics of Pipeline Buried in Soft Soil Under Transportation Loads* (Zhejiang University, 2004).
9. Yanjiang Xie. *Research on Dynamic Response of Buried Pipeline in Soft Soil Foundation Under Cyclic Loading* (Guizhou University, 2021).
10. Xu, M., Shen, D. & Rakitin, B. The longitudinal response of buried large-diameter reinforced concrete pipeline with gasketed bell and spig Ot joints subjected to traffic loading. *Tunn. Undergr. Space Technol.* **64**, 117–132 (2017).
11. Jiang, W. L. et al. Study on dynamic response of buried pipeline rolled by heavy vehicle based on co-simulation by ADAMS and ABAQUS. *J. Phys. Conf. Ser.* **2185**, 012018 (2022).
12. Song, L. F. et al. 3D slope reliability analysis besed on the intelligent response surface methodology. *Bull. Eng. Geol. Environ.* **80**, 735–749 (2021).
13. Kang, F. & Li, J. J. Artificial bee colony algorithm optimized support vector regression for system reliability analysis of slopes. *J. Comput. Civil Eng.* **30** (3), 04015040 (2016).
14. Kang, F., Xu, Q. & Li, J. J. Slope reliability analysis using surrogate models via new support vector machines with swarm intelligence. *Appl. Math. Model.* **40** (11–12), 6105–6120 (2016).

Acknowledgements

This research was supported by China National Natural Science Foundation (Grant no. 52325806, W2411045, 52378364, 52478357), Zhejiang Provincial Natural Science Foundation of China under (LTGG23E080003), Scientific Research Project of Wenzhou (ZS2023005), Wenzhou Ouyue Talent Program High level Innovation Team.

Author contributions

Laifu Song: Conceptualization, Methodology, Writing—original draft, Writing—review & editing. Hongtao Fu: Funding acquisition, Investigation. Jun Wang: Conceptualization, Funding acquisition, Writing—review & editing. Jiayu Cai: Writing—original draft, Investigation. Shun Zhang: Investigation.

Declarations

Competing interests

The authors declare no competing interests.

Additional information

Correspondence and requests for materials should be addressed to J.W.

Reprints and permissions information is available at www.nature.com/reprints.

Publisher's note Springer Nature remains neutral with regard to jurisdictional claims in published maps and institutional affiliations.